Multireference linearized coupled cluster theory for strongly correlated systems using matrix product states

Sandeep Sharma' and Ali Alavi'

Citation: The Journal of Chemical Physics **143**, 102815 (2015); doi: 10.1063/1.4928643
View online: http://dx.doi.org/10.1063/1.4928643
View Table of Contents: http://aip.scitation.org/toc/jcp/143/10
Published by the American Institute of Physics

Multireference linearized coupled cluster theory for strongly correlated systems using matrix product states

Sandeep Sharma[1,a)] and Ali Alavi[1,2,b)]
[1]*Max Planck Institute for Solid State Research, Heisenbergstraße 1, 70569 Stuttgart, Germany*
[2]*Department of Chemistry, University of Cambridge, Lensfield Road, Cambridge CB2 1EW, United Kingdom*

(Received 16 May 2015; accepted 29 July 2015; published online 24 August 2015)

We propose a multireference linearized coupled cluster theory using matrix product states (MPSs-LCC) which provides remarkably accurate ground-state energies, at a computational cost that has the same scaling as multireference configuration interaction singles and doubles, for a wide variety of electronic Hamiltonians. These range from first-row dimers at equilibrium and stretched geometries to highly multireference systems such as the chromium dimer and lattice models such as periodic two-dimensional 1-band and 3-band Hubbard models. The MPS-LCC theory shows a speed up of several orders of magnitude over the usual Density Matrix Renormalization Group (DMRG) algorithm while delivering energies in excellent agreement with converged DMRG calculations. Also, in all the benchmark calculations presented here, MPS-LCC outperformed the commonly used multi-reference quantum chemistry methods in some cases giving energies in excess of an order of magnitude more accurate. As a size-extensive method that can treat large active spaces, MPS-LCC opens up the use of multireference quantum chemical techniques in strongly correlated *ab initio* Hamiltonians, including two- and three-dimensional solids. [http://dx.doi.org/10.1063/1.4928643]

INTRODUCTION

One of the most pressing theoretical questions in electronic structure theory is how to deal with realistic strongly correlated electronic systems, which typically exhibit combinatorial complexity in the description of the ground-state wavefunction. There are two dominant paradigms in electronic structure algorithms, namely, *variational* and *projective* methods, which for different reasons struggle to capture the entirety of the problem. Variational methods (such as configuration interaction (CI)[1] and Density Matrix Renormalization Group (DMRG)[2,3]) are in principle robust techniques, but generally scale exponentially in the number of correlating orbitals and do not provide size-extensive energies (except in unreachable exact limits), whilst projective methods, such as many-body perturbation theory and coupled cluster theory, spectacularly successful in describing weak correlation, fail as the underlying single-reference wavefunction upon which they are build diminishes in importance with growing strength of correlation. It is natural to ask if a judicious combination of a variational method and a projective method exists which can tractably handle realistic strong-correlation systems. Here, we propose such a method that is based on the linearized Coupled-Cluster (LCC) method[4] and is implemented using the matrix-product states (MPSs)[5] formalism to capture highly multi-configurational zeroth- (and higher) order wavefunctions.

To give a consolidated presentation, we first start by deriving the governing equations for the single reference LCC method which uses the Hartree-Fock wavefunction as the zeroth order state. We show that LCC is closely related to the commonly used variational method, the configuration interaction with singles and doubles (CISD). We highlight the strengths and weaknesses of LCC compared to CISD. The main shortcoming of LCC (it becomes divergent when near-degeneracies are present) can be overcome by using a multireference zeroth order wavefunction. These multireference LCC equations have the same relation to the variational equations usually solved using DMRG,[6–11] as the LCC equations have CISD. We show how the matrix product states can be used to efficiently solve the multireference equations by a small modification of the DMRG algorithm, resulting in a method which we call MPS-LCC. The resulting method is extremely powerful and we demonstrate its strength by solving several tough paradigmatic benchmark problems: first-row dimers at equilibrium and stretched geometries, the 1-band and 3-band (cuprate-like) Hubbard models in the strong-correlation regime $U/t = 4 - 10$ and the Cr_2 dimer.

THEORY

To derive linearized coupled cluster equations, one starts with the coupled cluster singles and doubles wavefunction written using the exponential ansatz $|\Psi\rangle = e^{\hat{T}}|\Phi_0\rangle$, where $\hat{T} = \hat{T}_1 + \hat{T}_2$ is the sum of the single and double excitation operators and $|\Phi_0\rangle$ is the Hartree-Fock wavefunction. When the CC wavefunction is substituted into the Schrödinger equation $\hat{H}|\Psi\rangle = E|\Psi\rangle$ and is left multiplied by $e^{-\hat{T}}$, we obtain $e^{-\hat{T}}\hat{H}e^{\hat{T}}|\Phi_0\rangle = E|\Phi_0\rangle$. Left projecting onto the Hartree–Fock and a set of singly and doubly excited determinants $|\Phi_\mu\rangle$, we obtain the expression for the coupled cluster energy and the governing equations for the t–amplitudes,

$$E = \langle\Phi_0|e^{-\hat{T}}\hat{H}e^{\hat{T}}|\Phi_0\rangle, \quad (1)$$

$$0 = \langle\Phi_\mu|e^{-\hat{T}}\hat{H}e^{\hat{T}}|\Phi_0\rangle. \quad (2)$$

a)Electronic address: sanshar@gmail.com
b)Electronic address: a.alavi@fkf.mpg.de

The set of non-linear Equation (2) can be solved to evaluate the t–amplitudes which can then be substituted into Equation (1) to obtain the coupled cluster energy. To obtain LCC equations, the above equations can further be simplified by expanding the exponential using the Baker-Campbell-Hausdorff expansion and truncating the series at the first order, i.e., $e^{-\hat{T}}\hat{H}e^{\hat{T}} = \hat{H} + [\hat{H},\hat{T}]$, to yield

$$E = \langle\Phi_0|\hat{H}|\Phi_0\rangle + \langle\Phi_0|\hat{H}|\Psi_1\rangle, \tag{3}$$

$$0 = \langle\Phi_\mu|\hat{H}|\Phi_0\rangle + \langle\Phi_\mu|(\hat{H} - E_0)|\Psi_1\rangle. \tag{4}$$

Equations (3) and (4) are the governing equations of the single reference linearized coupled cluster theory, where we have defined that $|\Psi_1\rangle \equiv \hat{T}|\Phi_0\rangle$ is the LCC correction to the Hartree-Fock wavefunction consisting of only single and double excitations. Equation (4) is now a linear equation in the unknown $|\Psi_1\rangle$ which can be solved and substituted into Equation (3) to calculate the LCC energy.

Now let us recall that the variational principle can be written as a set of equations $\langle\Phi_\mu|H - E|\Psi\rangle = 0$, where $|\Phi_\mu\rangle$ are the basis states used to expand the wavefunction $|\Psi\rangle$. When the variational principle is used to optimize the CISD wavefunction, we obtain

$$E = \langle\Phi_0|\hat{H}|\Phi_0\rangle + \langle\Phi_0|\hat{H}|\Psi_1\rangle, \tag{5}$$

$$0 = \langle\Phi_\mu|\hat{H}|\Phi_0\rangle + \langle\Phi_\mu|(\hat{H} - E)|\Psi_1\rangle, \tag{6}$$

where we have used intermediate normalization ($\langle\Phi_0|\Psi\rangle = 1$) and as before $|\Psi_1\rangle$ is the correction to the Hartree-Fock wavefunction consisting of only singly and doubly excited determinants. These equations are remarkably similar to Equations (3) and (4) with the small modification that the zeroth order energy E_0 in Equation (4) is replaced with the variational energy E in Equation (6). This seemingly small change has a significant implication that the LCC energies unlike the CISD energies are fully size-extensive. The LCC energies are nearly equal to the full CCSD energies for weakly correlated problems. We demonstrate this by showing the correlation energy of diamond in Table I with an *ab initio* Hamiltonian on a $2 \times 2 \times 2$ k–point sampling resulting in 64 electrons in 64 orbital problem (see Ref. 12 for more details).

The size-extensivity unfortunately comes at the cost of variationality and more problematic is the fact that the equations are prone to divergence[13] in cases of near degeneracy when other determinants besides the Hartree-Fock have energies similar to E_0.

This shortcoming can be overcome by formulating a multireference LCC method in which the E_0 and Ψ_0 in Equation (4) are replaced by the energy and wavefunction obtained by fully correlating a set of orbitals around the Fermi surface. Such a multireference LCC method has been formally derived in the past by Bartlett *et al.*[14,15] as well as by Fink.[16,17] Here, we use Fink's formulation in which the single reference LCC is written as a perturbation theory using an ingenious use of a zeroth order Hamiltonian. This perturbation theory is then straightforwardly extended to multireference cases thus resulting in a multireference LCC theory. The advantage of Fink's formulation is that it not only reduces to the LCC equations at the first order but systematic higher order corrections can also be generated.

TABLE I. The correlation energy (E_h/electron) of diamond calculated using various theories with an *ab initio* Hamiltonian. The DMRG calculation is still very far from convergence even though it was performed using a MPS with a large virtual bond dimension of $M = 7500$. The LCC energies are of comparable accuracy to the CCSD and the FCIQMC energies and were calculated using a small MPS with $M = 500$, representing a speed up of over 3 orders of magnitude over the DMRG calculation. (See the main text for algorithmic details.)

FCIQMC	MP2	CCSD	LCC	DMRG
−0.6190	−0.5145	−0.6134	−0.6235	−0.5477

Following Fink's formulation, we first start by dividing all the orbitals into an active (or correlating) set, in which the orbital occupancies can be 0,1,2, a core set in which the occupancies are constrained to be 2, and a virtual set with zero occupancy. Then, we partition the full Hamiltonian $\hat{H}$, whose ground-state wavefunction Ψ we seek, in terms of number-preserving operators within each subset,

$$\hat{H} = \sum_{ij} t_{ij} a_i^\dagger a_j + \sum_{ijkl} \langle ij|kl\rangle a_i^\dagger a_j^\dagger a_l a_k = \hat{H}_0 + \hat{U}, \tag{7}$$

$$\hat{H}_0 = \sum_{\substack{ij;\\ \Delta n_{ex}=0}} t_{ij} a_i^\dagger a_j + \sum_{\substack{ijkl;\\ \Delta n_{ex}=0}} \langle ij|kl\rangle a_i^\dagger a_j^\dagger a_l a_k. \tag{8}$$

The constraint $\Delta n_{ex} = 0$ implies that the operators do not transfer electrons between the three sets of orbitals, and $\hat{U}$ contains all remaining terms.

To begin with, we will assume that the ground-state eigenfunction $\Phi^{(0)}$ of $\hat{H}_0$ can be found (later, this assumption will be relaxed using the *projector* approximation). This zeroth order wavefunction (which will, in general, have a combinatorial complexity) has an eigenvalue equal to the expectation value of the full Hamiltonian $E^{(0)} = \langle\Phi^{(0)}|H|\Phi^{(0)}\rangle$ and the first order energy is zero. It is possible to develop the usual perturbation theory master equations to express successive corrections ($\Phi^{(n)}$) to the wavefunction: $\Psi = \Phi^{(0)} + \Phi^{(1)} + \Phi^{(2)} + \cdots$. We expect this series to converge if the norms at each subsequent order rapidly diminish. In the limit in which the active space spans all orbitals, we recover full CI (which is always convergent), whereas in the opposite limit where there are zero orbitals in the active space, we recover linearized coupled cluster theory, itself an excellent weak-correlation theory, but which diverges in strong correlation systems. We expect to have convergent theory for any level of correlation as long as the active space is sufficiently large.

The equations governing $\Phi^{(n)}$ are shown in Equation (9), where P is the projector on to the zeroth order wavefunction ($P = |\Phi^{(0)}\rangle\langle\Phi^{(0)}|$) and Q is its complement ($1 - P$); the set of linear equations must be solved one at a time to obtain the n^{th} order correction to the wavefunction ($\Phi^{(n)}$).[18] Once $\Phi^{(n)}$ is known, $2n$ and $2n + 1$ order corrections to the energy (E^{2n}, E^{2n+1}) can be calculated due to Wigners $(2n + 1)$ rule using Equation (10),

$$(\hat{H}_0 - E^{(0)})|\Phi^{(n)}\rangle = Q\left(-\hat{U}|\Phi^{(n-1)}\rangle + \sum_{k=1}^{n} E^{(k)}|\Phi^{(n-k)}\rangle\right), \tag{9}$$

$$E^{(2n)} = \langle \Phi^{(n-1)} | \hat{U} | \Phi^{(n)} \rangle - \sum_{k=1}^{n} \sum_{j=1}^{n-1} E^{(2n-k-j)} \langle \Phi^{(k)} | \Phi^{(j)} \rangle,$$

$$E^{(2n+1)} = \langle \Phi^{(n)} | \hat{U} | \Phi^{(n)} \rangle - \sum_{k=1}^{n} \sum_{j=1}^{n} E^{(2n+1-k-j)} \langle \Phi^{(k)} | \Phi^{(j)} \rangle. \quad (10)$$

We use the variational principle for the perturbation theory[19,20] which states that to solve Equation (9), it is sufficient to minimize the Hylleraas functional shown in Equation (14) with respect to $|\Phi^{(n)}\rangle$. Only a small modification to the DMRG algorithm, implemented in the Block code,[21–23] was required to minimize the Hylleraas functional. The details of the algorithm are outlined in the section titled Implementation.[24]

Projector approximation: The cost of optimizing the zeroth order wavefunction scales exponentially with the size of the active space. This exponential cost can be circumvented by only approximately diagonalizing the zeroth order Hamiltonian. The error in the zeroth order wavefunction can then also be corrected perturbatively. To do this, we define a new zeroth-order Hamiltonian $\tilde{H}_0 = P\hat{H}_0 P + Q\hat{H}_0 Q$, and the perturbing Hamiltonian becomes $\tilde{U} = P\hat{H}_0 Q + Q\hat{H}_0 P + \hat{U}$. It can then be shown that the use of the modified zeroth order Hamiltonian changes Equation (9) only at the first order to $(\hat{H}_0 - E^{(0)})|\Phi^{(1)}\rangle = Q\hat{H}|\Phi^{(0)}\rangle$, where $\hat{H}$ is the unperturbed Hamiltonian; and the expression of the second order energy changes from $\langle \Phi^{(0)} | \hat{U} | \Phi^{(1)} \rangle$ to $\langle \Phi^{(0)} | \hat{H} | \Phi^{(1)} \rangle$. These results are remarkable because in essence they imply that even approximate solution of the zeroth order equation is sufficient and the original perturbation series can be used with only minor modifications.

Before moving on to describe our implementation, we would like to point out that Fink's formulation is different than Bartlett's formulation of LMRCC theory. Unlike Bartlett's equations,[15] in Fink's equations the states with different number of electrons in the active, core and virtual spaces don't interact with each other through the zeroth order Hamiltonian. Also, unlike Bartlett's equations the present LMRCC equations cannot be obtained straightforwardly from governing equations of ic-MRCC[25,26] by discarding terms that are higher order than linear in the excitation operator T. A key difference between our the current approach and the commonly used approach in multireference methods is that we use a single MPS to represent the first order wave function instead of expanding it in the space formed by internally contracted singles and doubles excitations out of the reference wavefunction. The states forming this space are not mutually orthogonal and without special care the equations can become ill-conditioned due to linear dependencies. The problem of linear-dependencies never arises in our formulation, further unlike the usual formulations at convergence our wavefunction is allowed to relax in the full uncontracted space of singles and doubles excitations. Another important difference is that unlike the usual formulation, we do not need any reduced density matrices, for example, up to sixth-order reduced density matrices (RDMs) are required for a naive implementation of ic-MRCI calculations, although in practice, this requirement can be relaxed by using configuration state functions instead of internally contracted states.[27,43] The two other approaches used for incorporating post-DMRG dynamical correlation are the canonical transformation theory and the methods based on exploring the tangent space of the MPS.[28–30] The canonical transformation theory[31,32] tries to perform the unitary multireference coupled cluster theory, but with the simplification that all RDMs higher than the two-body RDMs are evaluated using the cumulant approximation. The tangent space based methods are, in principle, quite similar to our current method with the main difference that the corrections to the reference MPS are restricted to linear combination of its tangent space vectors. This is a far more restrictive space than the one used here which is the one spanned by a single MPS with an arbitrarily large bond dimension.

We would also like to emphasize that this method can be extended in several ways. First, the static one-particle and two-particle correlation functions of the ground state can be easily calculated.[33,34] Second, in addition to the ground state, a set of low-lying excited states can also be calculated with a computational cost that scales linearly with the number of states using quasi-degenerate perturbation theory.[35–37] Finally, dynamical correlation functions can be calculated by combining the working equations of coupled cluster Green's function framework[38] with the dynamical DMRG.[39,40]

IMPLEMENTATION

A general MPS representing a wavefunction $|\Psi\rangle$ is shown in Eq. (12), where n_i is the occupation of orbital i, and $i_1 \ldots i_{k-1}$ are the virtual indices that are contracted to obtain the final state. By increasing the size of the virtual indices, a MPS can be used to represent any wavefunction arbitrarily accurately. Similarly, operator Ω can be written in a matrix product operator (MPO) form as shown in Eq. (13). It should be noted that the expression in Equation (13) is very general, but it can be simplified if one limits the operator to have at most two body interactions. In such cases, it can be shown that the virtual bond dimension of the operator needs never be greater than k^2, where k is the number of orbitals. The algebraic notation very quickly becomes cumbersome due to the rapid proliferation of indices; instead, the graphical notation which is briefly explained below is much more convenient and intuitive. Here, we can only give a short introduction to the notation, for more details we refer the reader to the excellent review article by Schollwöck.[5]

Both the MPS and MPO can be conveniently represented graphically as shown in Figure 1. In the figures, each matrix (strictly speaking this is a three dimensional tensor) of the MPS is represented by a circle with three bonds jutting out, one pointing in the upward direction which corresponds to the physical index n_i and two others pointing horizontally that correspond to the virtual indices. The bonds corresponding to the virtual indices of the adjacent matrices are joined together, which algebraically corresponds to contracting the virtual indices, to obtain the wavefunction. The different MPS and MPO when written graphically are distinguished by the symbols used to represent their matrices; for example, here, we use a circle of Ψ, a triangle for Φ, and a square for H_0, respectively.

It can be shown that taking the overlap between two MPS and calculating the matrix element of a MPO between two

MPS can be performed with a polynomial cpu cost of $O(kM^3)$ and $O(k^3M^3)$, respectively (see Figure 2). To get this computational scaling, one needs to perform the various tensor contractions in a specific well-defined order. A suboptimal order of contractions can lead to computational cost that scales exponentially with the number of orbitals k. The partial derivative of overlap or operator expectation value with respect to one of the matrices of a MPS gives rise to a tensor which has exactly the same dimension as that of the matrix. This partial derivative in graphical language is represented by graph of the overlap or the expectation with the corresponding matrix removed from it as shown in Figure 3. In both MPS-LCC and DMRG, the functional being optimized is quadratic in the wavefunction of interest. In the case of DMRG, it is the energy functional,

$$E[\Psi] = \langle\Phi|\hat{H}|\Phi\rangle - \langle\Phi|E|\Phi\rangle \tag{11}$$

and in the case of LCC, it is the Hylleraas functional shown in Equation (14),

$$|\Psi\rangle = \sum_{\{n\},i_1\ldots i_{k-1}} A^{n_1}_{i_1} A^{n_2}_{i_1 i_2} \ldots A^{n_k}_{i_{k-1}} |n_1 n_2 \ldots n_k\rangle, \tag{12}$$

$$\Omega = \sum_{\{n\}\{n'\},i_1\ldots i_{k-1}} W^{n_1 n'_1}_{i_1} W^{n_2 n'_2}_{i_1 i_2} \ldots W^{n_k n'_k}_{i_{k-1}} |n_1 n_2 \ldots n_k\rangle\langle n'_1 n'_2 \ldots n'_k|, \tag{13}$$

$$H[\Phi^{(n)}] = \langle\Phi^{(n)}|\hat{H}_0 - E^{(0)}|\Phi^{(n)}\rangle - \left(\langle\Phi^{(n)}|\hat{U}|\Phi^{(n-1)}\rangle - \sum_{k=1}^{n} E^{(k)}\langle\Phi^{(n)}|\Phi^{(n-k)}\rangle\right) + \langle\Phi^{(n)}|\Phi^{(0)}\rangle\left(\langle\Phi^{(0)}|\hat{U}|\Phi^{(n-1)}\rangle - \sum_{k=1}^{n} E^{(k)}\langle\Phi^{(0)}|\Phi^{(n-k)}\rangle\right). \tag{14}$$

In MPS-LCC, the wavefunction of interest is written as a MPS and is then evaluated by minimizing the Hylleraas functionals using the sweep algorithm. The key element of the sweep algorithm is that at each sweep iteration l, only one tensor $A^{n_l}_{i_{l-1}i_l}$ is optimized keeping all the others constant. Figure 3 shows the partial derivative of $\langle\Psi|\Phi\rangle$ and $\langle\Psi|H|\Phi\rangle$ with respect to the unknown tensor $A^{n_l}_{i_{l-1}i_l}$ of wavefunction Ψ. The governing equations that need to be solved at each sweep iteration are obtained by taking the partial derivatives of Equation (14) and equating them to zero. This converts a complicated multi-linear problem into a linear algebra problem (a linear equation) with the elements of tensor $A^{n_l}_{i_{l-1}i_l}$ as unknowns. Standard iterative algorithms like the Jacobi-Davidson and conjugate-gradient methods can be used to solve the linear algebra problems. By increasing the virtual bond dimension of the MPS expressing $|\Phi^{(n)}\rangle$, Equation (14) can be minimized arbitrarily accurately. The cpu cost per sweep iteration for calculating the two most expensive terms $|\langle\Phi^{(n)}|\hat{H}_0 - E^{(0)}|\Phi^{(n)}\rangle$ and $\langle\Phi^{(n)}|\hat{U}|\Phi^{(n-1)}\rangle$ on the right hand size of Equation (14) is $O(k^2M_n^3)$ and $O(k^2M_n^2M_{n-1})$ + $O(k^2M_nM_{n-1}^2)$, respectively, where M_n is the virtual bond dimension of the MPS representing the state $|\Phi^{(n)}\rangle$. The entire algorithm is implemented in the Block code which includes the ability to treat several different symmetries including $SU(2)$ and non-abelian point group.

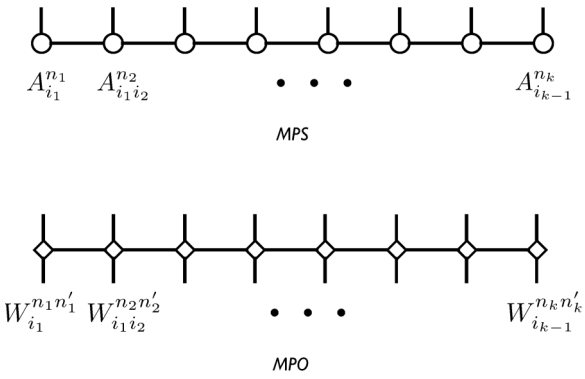

FIG. 1. A matrix product state (MPS) can be represented graphically using a series of 3-dimensional tensors in which, the physical index (pointing upwards) of the tensors denotes the occupation of the orbital and the other two indices, known as virtual indices, are sequentially contracted. Similarly, a matrix product operator (MPO) can be represented graphically using a series of 4-dimensional tensors, with two physical indices and two virtual indices. The virtual indices of adjacent tensors are contracted sequentially.

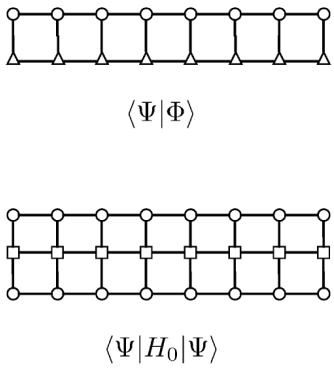

FIG. 2. The figure shows the overlap and a transition matrix element of a MPO H_0 between MPS Ψ and Φ. These are calculated by contracting the free physical dimension of the MPS and MPO sequentially as shown in the figure. By appropriately ordering the sequence of these contractions, it can be shown that the cost of evaluating an overlap is $O(kM^3)$ and a transition matrix element is $O(k^3M^3)$, respectively.

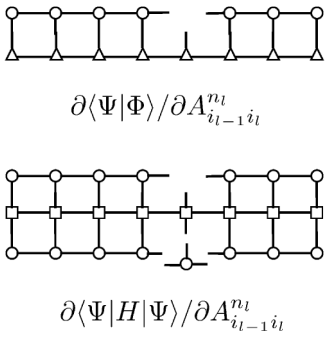

FIG. 3. The figure shows the partial derivative of the overlap and transition matrix element with respect to the local tensor $A^{n_l}_{i_{l-1}i_l}$ of the MPS. Each of these graphs represents $4M^2$ terms corresponding to taking the partial derivative with respect to each element of the tensor $A^{n_l}_{i_{l-1}i_l}$.

BENCHMARKS

Earlier we showed that MPS-LCC is more efficient than the variational DMRG algorithm for weakly correlated systems like the diamond crystal. Here, we demonstrate that it shows equally impressive performances for first row dimers at equilibrium and stretched geometries, strongly correlated systems like 2-dimensional 1-band and 3-band Hubbard model at half-filling and the Cr_2 dimer. The half filled 1-band Hubbard model is chosen because reliable auxiliary-field quantum Monte Carlo (AFQMC) results are available due to absence of sign-problem. It should be pointed out that from the perspective of MPS-LCC calculations, half-filling represents the hardest case and we expect the quality of results to be better away from half-filling.

First row dimers

We start by calculating the energy of the ground state of the C_2 dimer at various bond lengths using MPS-LCC with the double-zeta basis set. The MPS-LCC calculations are performed on a multi-configuration self consistent field (MCSCF) reference wavefunction with an active space of (8o, 8e) and the resulting energies are tabulated in Table II. The table also shows the full configuration interaction (FCI) energies which are calculated by correlating all 12 electrons in 28 orbitals using the DMRG algorithm as implemented in the Block code. The errors in the MCSCF and MPS-LCC energies, calculated relative to the FCI energies, are plotted in Figure 4. We see that there is a discontinuity in the MCSCF and MPS-LCC energies at a bond length of 3.10 bohrs. This is because the $^1\Sigma_g^+$ and $^1\Delta_g$ energy curves cross between 3.05 bohrs and 3.10 bohrs bond lengths, with the former being the ground state at shorter bond lengths and the latter being the ground state at larger bond lengths. In our calculations, the discontinuity in the MCSCF and MPS-LCC curves arises because we have only used the D_{2h} subgroup of the full $D_{\infty h}$ point group of the molecule. Besides the discontinuity at the curve crossing, the MPS-LCC energy is both continuous and smooth despite the fact that at bond lengths greater than 3.05 bohrs, the ground state and the first excited states are nearly degenerate with a maximum separation of less than 6 mE_h.

We also benchmark the MPS-LCC method for C_2, N_2, and F_2 molecules at their equilibrium bond lengths of 1.242 53, 1.0977, and 1.4119 Å, respectively, against the FCI energies calculated using the full-configuration interaction quantum Monte Carlo (FCIQMC) method with up to quadruple-zeta basis set.[41] Here, the energies are calculated using various commonly used active-space methods like

TABLE II. The table shows the ground state energy of the C_2 dimer calculated using various methods with the cc-pVDZ basis set. The MCSCF and MPS-LCC use (8e, 8o) active space and the FCI energy is calculated by fully correlating 12 electrons in 28 orbitals.

	Energy/E_h		
r/a_0	FCI	MCSCF	MPS-LCC
1.80	−75.4549	−75.3501	−75.4532
1.85	−75.5132	−75.4080	−75.5116
1.90	−75.5621	−75.4564	−75.5605
1.95	−75.6026	−75.4965	−75.6010
2.00	−75.6358	−75.5294	−75.6343
2.05	−75.6628	−75.5560	−75.6613
2.10	−75.6843	−75.5771	−75.6828
2.15	−75.7010	−75.5935	−75.6996
2.20	−75.7136	−75.6058	−75.7122
2.25	−75.7227	−75.6145	−75.7213
2.30	−75.7287	−75.6202	−75.7272
2.35	−75.7320	−75.6232	−75.7306
2.40	−75.7332	−75.6240	−75.7317
2.45	−75.7324	−75.6229	−75.7309
2.50	−75.7300	−75.6202	−75.7285
2.55	−75.7263	−75.6161	−75.7247
2.60	−75.7215	−75.6109	−75.7199
2.65	−75.7159	−75.6047	−75.7141
2.70	−75.7095	−75.5979	−75.7076
2.75	−75.7026	−75.5904	−75.7006
2.80	−75.6953	−75.5825	−75.6931
2.85	−75.6878	−75.5743	−75.6853
2.90	−75.6802	−75.5659	−75.6773
2.95	−75.6726	−75.5573	−75.6693
3.00	−75.6652	−75.5487	−75.6612
3.05	−75.6580	−75.5400	−75.6532
3.10	−75.6512	−75.5208	−75.6509
3.15	−75.6467	−75.5163	−75.6464
3.20	−75.6420	−75.5116	−75.6418
3.25	−75.6373	−75.5068	−75.6371
3.30	−75.6326	−75.5020	−75.6323
3.35	−75.6278	−75.4972	−75.6276
3.40	−75.6230	−75.4924	−75.6228
3.45	−75.6183	−75.4877	−75.6182
3.50	−75.6137	−75.4831	−75.6135
3.55	−75.6091	−75.4785	−75.6090
3.60	−75.6047	−75.4740	−75.6046
3.65	−75.6003	−75.4696	−75.6002
3.70	−75.5961	−75.4654	−75.5960
3.75	−75.5920	−75.4613	−75.5920
3.80	−75.5880	−75.4573	−75.5880
3.85	−75.5842	−75.4535	−75.5842
3.90	−75.5805	−75.4498	−75.5805
3.95	−75.5769	−75.4463	−75.5770
4.00	−75.5735	−75.4429	−75.5737
4.05	−75.5703	−75.4398	−75.5705
4.10	−75.5672	−75.4367	−75.5674
4.15	−75.5642	−75.4339	−75.5645

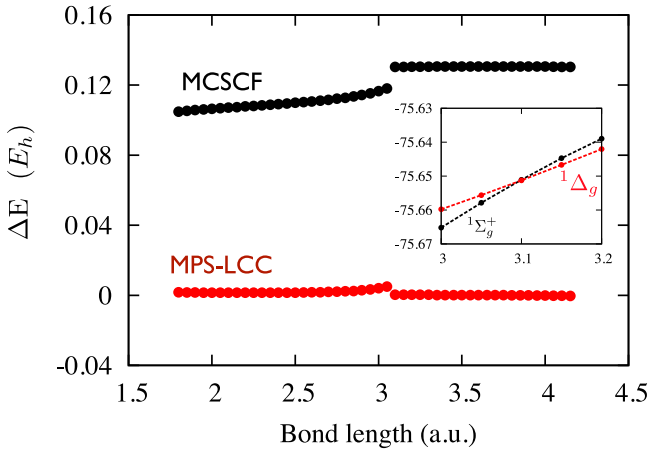

FIG. 4. The figure shows the error in the energies calculated using MCSCF and MPS-LCC methods relative to the FCI energies for the carbon dimer at various bond lengths using the cc-pVDZ basis set. There is a discontinuity in the energies of the MPS-LCC and MCSCF methods at 3.1 bohrs because of a curve crossing between $^1\Sigma_g^+$ and $^1\Delta_g$ states. This curve crossing is shown in the inset.

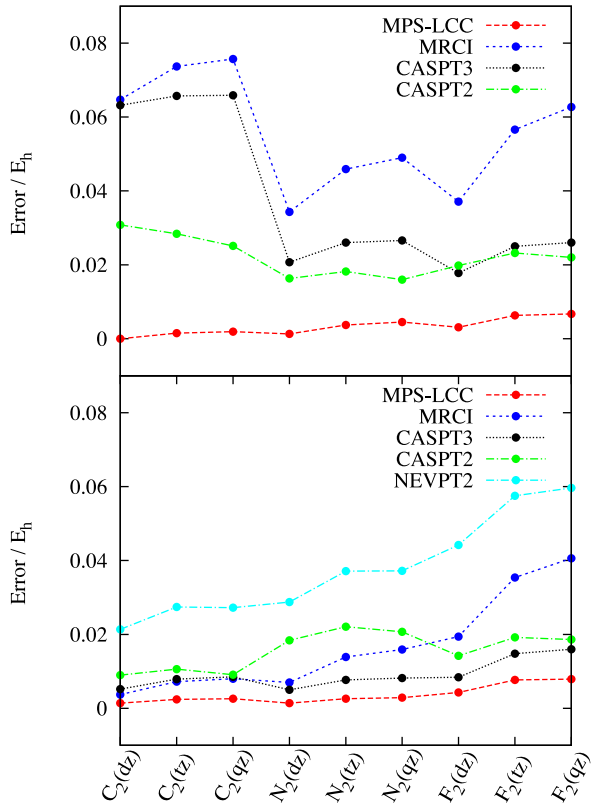

FIG. 5. The error in the energies calculated using various active space methods relative to the highly accurate FCIQMC energies[41] of C_2, N_2, and F_2 molecules at bond lengths of 1.242 53, 1.0977, and 1.4119 Å, respectively. The upper panel shows the errors when the CAS-CI wavefunction was the reference and the bottom panel used a MCSCF wavefunction as reference. In both cases, the active space chosen was the full valence space containing eight orbitals.

MRCI,[42,43] CASPT2, CASPT3,[44] NEVPT2,[45,46] and the MPS-LCC method developed in this work. For all these methods, two sets of calculations were performed, the first in which a complete active space configuration interaction (CAS-CI) wavefunction was used as a reference and in the second MCSCF wavefunction was used. Both CAS-CI and MCSCF calculations were performed with frozen core and all the valence orbitals included in the active space. The results of the calculations are shown in Table III and are plotted in Figure 5. These calculations show that MPS-LCC gives higher accuracy for these molecules compared to all other methods. One striking feature of these results is the fact that the quality of the MPS-LCC results is almost unaffected by the reference wavefunction. This is a well known feature of the CCSD method, but from these results, it looks like the linearized version of the theory also shows this feature as long as the active space is large enough to avoid divergences.

It can be seen that the results of the MRCI calculation for the F_2 dimer are much less accurate than the C_2 and N_2 dimers. This is most likely due to the relatively small size of the zeroth order wavefunction which only has about 64 determinants in the active space compared to 4900 and 3136 determinants, respectively, for C_2 and N_2, respectively. The perturbation theories are in general somewhat less sensitive to the size of the Hilbert space of the zeroth order wavefunction because they are not variational.

We have also performed calculations on the C_2 dimer with cc-pVQZ basis set at various bond lengths shown in

TABLE III. The third column shows the ground state energy and estimated uncertainty in Hartrees (E_h) of the C_2, N_2, and F_2 molecules at bond lengths of 1.242 53, 1.0977, and 1.4119 Å, respectively, calculated using the FCIQMC[41] method. The rest of the table shows the errors of various active space methods relative to FCIQMC in milli-Hartrees (mE_h). The active space used for these calculations consisted of the eight valence orbitals including $2s$ and $2p$ orbitals. Two sets of calculations were performed, one with the CAS-CI reference and the other with MCSCF reference.

		FCIQMC	CAS-CI reference (mE_h)				MCSCF reference (mE_h)				
Molecule	Basis	(E_h)	MPS-LCC	CASPT2	CASPT3	MRCI	MPS-LCC	CASPT2	CASPT3	MRCI	NEVPT2
C_2	dz	−75.7285(1)	0.0	64.7	30.8	63.2	1.4	9.0	5.2	3.7	21.4
C_2	tz	−75.7850(1)	1.5	73.7	28.4	65.7	2.4	10.6	7.9	7.2	27.4
C_2	qz	−75.8023(3)	1.9	75.7	25.1	65.9	2.6	9.1	8.5	8.0	27.2
N_2	dz	−109.2767(1)	1.3	34.3	16.3	20.7	1.4	18.4	5.0	7.0	28.7
N_2	tz	−109.3754(1)	3.7	45.9	18.2	26.0	2.6	22.1	7.7	13.9	37.1
N_2	qz	−109.4058(1)	4.5	49.0	16.0	26.6	2.9	20.7	8.2	15.9	37.2
F_2	dz	−199.0994(1)	3.1	37.1	19.8	17.8	4.3	14.2	8.4	19.4	44.2
F_2	tz	−199.2977(1)	6.3	56.6	23.2	25.0	7.7	19.2	14.8	35.4	57.5
F_2	qz	−199.3598(2)	6.7	62.7	22.0	26.0	7.9	18.6	16.0	40.6	59.6

TABLE IV. The second row of the table shows the DMRG energy in Hartrees for carbon dimer at various bond lengths. The rest of the table shows the error in milli-Hartree (mE_h) of various methods relative to the DMRG energies. All calculations besides DMRG were performed on a reference wavefunction obtained by a frozen core MCSCF calculation with eight electrons in eight orbitals active space.

r	DMRG	MPS-LCC	MRCI	CASPT3	CASPT2	NEVPT2
(Å)	(E_h)			(mE_h)		
1.1	−75.7613	2.7	8.2	7.7	9.7	27.9
1.2	−75.7992	2.8	8.3	8.5	9.5	27.7
1.242 53	−75.8027	2.3	8.4	8.9	9.5	27.6
1.3	−75.7994	3.2	8.5	9.5	9.5	27.6
1.4	−75.7797	3.9	9.1	10.9	9.8	28.0
1.6	−75.7241	0.1	12.4	5.7	22.8	27.2
2	−75.6460	1.6	8.4	7.6	15.4	29.0

Table IV. Here, the accurate benchmark data are obtained using the frozen core DMRG calculations[23] published recently. These results are plotted in Figure 6 and again show the higher accuracy obtained by the MPS-LCC method relative to other methods. There are larger non-parallality errors at bond length of 1.6 Å possibly because of curve crossing between two A_g states (the intersecting $^1\Sigma_g^+$ and $^1\Delta_g$ states belong to the A_g irreducible representation in the D_{2h} subgroup) near this geometry. Quasi-degenerate perturbation theory can, in principle, be used to ameliorate these problems.

Cr2 dimer

The chromium dimer has been a challenging problem for quantum chemistry and large active spaces and basis sets are required to obtain the correct binding curve.[47–57] Here, we do not try to calculate the best binding curve that we can, but instead use some smaller benchmark calculations to compare the commonly used quantum chemical methods against the MPS-LCC method. In particular, we carry out an all electron (48e, 42o) calculation on the Cr_2 dimer with Ahlrichs and Schafer's SVP basis set at a bond length of 1.5 Å.

Table V shows the total energy and the well depth calculated using various quantum chemical methods, including coupled cluster with up to fourth order excitation and the

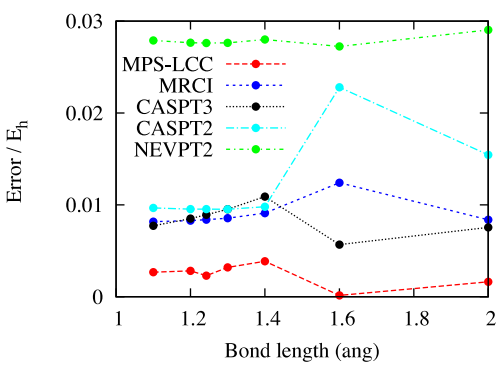

FIG. 6. The error in the energies of the carbon dimer using various active space methods relative to the energy calculated using DMRG which themselves have an error of less than 0.1 mH relative to the FCI energies.[23]

TABLE V. The table presents the absolute energies and the well depths (in E_h) calculated for the chromium dimer at 1.5 Å bond length with a SVP basis set. CASSCF, MRCI, and MPS-LCC theories used an active space of 12 electrons in 12 orbitals. Notice that the well-depth calculated using the MPS-LCC method is over an order of magnitude more accurate than the result of any other method presented. The "FCI" energy was calculated by extrapolating a large DMRG calculation[59] to zero discarded weight limit and is estimated to have a residual error of about 2 mE_h.

	1.5 Å (SVP)	
Method	Energy	Well depth
CASSCF	−2086.2256	0.167
CCSD	−2086.3880	0.177
CCSD(T)	−2086.4222	0.150
CCSDTQ	−2086.4302	0.143
MRCIC	−2086.4280	0.138
MPS-LCC	−2086.4349	0.129
FCI	−2086.4448 ± 0.002	0.129

contracted MRCI method[27] as implemented in Molpro.[58] All the multireference calculations including the LCC were performed with a zero order wavefunction obtained by performing a (12e,12o) CASSCF calculation. The first order MPS-LCC wavefunction was represented with a MPS of virtual bond dimension 4000. It can be seen that the MPS-LCC method not only gives a total energy closest to our best guess of FCI energy but the error in the calculated well depth is over an order of magnitude more accurate than any of the other methods shown here.

2d Hubbard model

We first calculate the ground state energy of a half filled 18-site 2D Hubbard lattice at $U/t = 4.0$. In this system, when 8 orbitals (4 degenerate orbitals above and 4 below the Fermi surface in k–space) are treated variationally and the rest of the orbitals are correlated using the MPS-LCC framework, we get excellent agreement with the AFQMC results which are expected to agree with the FCI results to all shown significant digits. The zeroth order wavefunction calculated variationally only captures about 14% of the correlation energy, but with the inclusion of the first order correction to the wavefunction, we account for 101% of the remaining correlation energy. Even though we do not necessarily recommend performing higher order perturbation theory, for illustration purposes, we show that subsequent higher order corrections calculated up to the 7th order show rapid converge towards the FCI energy as shown in Table VI. To access the cost of the method, we show in Figure 7 that the third order MPS-LCC energy rapidly converges to its final value with a MPS bond dimension (M) of only about 200. This is to be contrasted with the extremely slow convergence of DMRG algorithm with both localized and delocalized k–space basis. Given that the cpu time of both the MPS-LCC and the DMRG algorithm scale as $O(M^3)$, we see about three orders of magnitude improvement in the computational cost.

Now we assess the performance of the *projector approximation*, where the zeroth order wavefunction is only

TABLE VI. The table shows the results of a MPS-LCC and p–MPS-LCC calculations (energy/electron in units of t) to various orders of perturbation theory. For the 50 site Hubbard model, we have performed two MPS-LCC calculations, one with an active space of 8 electrons in 8 orbitals (p–MPS-LCC(8)) and the other with 24 electrons in 24 orbitals (p–MPS-LCC(24)). We have also shown the coupled cluster results up to the CCSDTQP level, calculated using the program MRCC[60,61] for the 18 site Hubbard model (the CC calculations did not converge for the 50 site Hubbard model).

	18 site 2D Hubbard			50 site 2D Hubbard	
Order of theory	MPS-LCC	p–MPS-LCC	CC	p–MPS-LCC(8)	p–MPS-LCC(24)
0	−0.804	−0.802	−0.778	−0.679	−0.705
2	−0.949	−0.948	−0.959	−0.873	−0.867
3	−0.960	−0.961	−0.965	−0.867	−0.878
4	−0.959	−0.960	−0.958	…	…
5	−0.958	−0.959	−0.958	…	…
6	−0.958	−0.958	…	…	…
7	−0.958	−0.958	…	…	…
FCI		−0.958[a]		−0.880[b]	

[a]Obtained by exact diagonalization.
[b]Auxiliary-field Monte Carlo,[62] which has no sign problem at half-filling.

approximately evaluated. Here, again the perturbation theory shows rapid convergence towards the FCI energy. In particular, when the energy of $\Psi^{(0)}$ is minimized by using a MPS with a virtual bond dimension of only 20 the errors in energy compared to full MPS-LCC rapidly diminish as shown in Table VI.

Two p–MPS-LCC calculations, one with (8e, 8o) and other with (24e, 24o) active space were performed on a 2-D Hubbard model with 50 sites. The zeroth order wavefunction in the two cases only accounted for about 1% and 14% of correlation energy, respectively. But remarkably, the third order correction to the energy was able to capture 95% and 99% of the remaining correlation energy. The first order correction to the wavefunction in the two cases above was represented by a MPS of bond dimension 5000 and 20 000, respectively. Based on the results of the smaller 18 site Hubbard model, we expect this perturbation theory to be rapidly convergent although it was not possible to carry out these calculations due to the high computational cost.

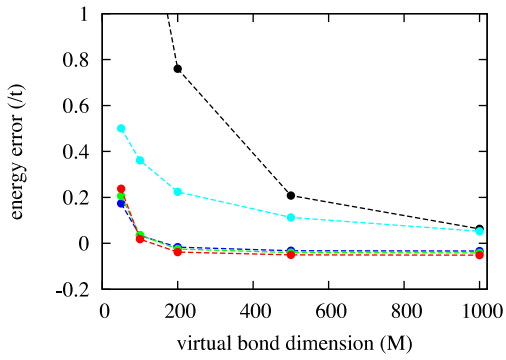

FIG. 7. The graph shows the energy error of three p-MPS-LCC calculations (where the approximate zeroth order wavefunction is represented with a MPS of bond dimension 100 (blue), 20 (green), and 10 (red), respectively) relative to the FCI energy versus the MPS bond dimension of the first order wavefunction. We have also shown the energy error of the DMRG calculation using localized orbitals (black) and delocalized k-space orbitals (cyan), respectively. The MPS-LCC method shows several orders of magnitude speed up over the corresponding DMRG calculations.

TABLE VII. Table shows the calculated ground state energy for the 3-band Hubbard model. Here, E_0 is the zeroth order energy obtained by fully correlating 10 holes in the 10 lowest energy orbitals. It is remarkable that the relatively much cheaper MPS-LCC theory is accurate to 4 significant places compared to the expensive DMRG calculation.

FCIQMC	E_0	MPS-LCC	DMRG
−1.5817(5)	1.3399	1.5821	1.5819

3-band Hubbard model

Recently Schwarz *et al.*[63] have published FCIQMC[64,65] results on an undoped 3-band ($p-d$) Hubbard model with 10 unit cells. Each unit cell containing CuO_2 is represented by three orbitals, one $3d_{x^2-y^2}$ centered on the Cu atom and a $2p_x$ and $2p_y$ orbital on the Oxygen atoms displaced in the x–direction and y–directions relative to the Cu, respectively. For the details of the Hamiltonian, we refer the reader to the original publication, but we would like to note that the model has inter-site potential and is extremely strongly correlated with the on-site repulsion divided by nearest neighbor hopping $U/t \approx 8$. We performed a MPS-LCC calculation, where 10 holes were exactly correlated in the 10 lowest energy orbitals and the effect of the remaining 20 orbitals was taken into account perturbatively with a first order wavefunction represented by a MPS of bond dimension $M = 1500$. Table VII shows that the resulting MPS-LCC energy has an astonishingly small error of less than 0.0002 eV/hole compared to a very large DMRG calculation with an $M = 6000$.

CONCLUSION AND OUTLOOK

In this paper, we show that the governing equations of multireference LCC theory can be efficiently solved using MPS by slightly modifying the DMRG algorithm. The theory has been used to obtain highly accurate energies, with a fraction of the cost of a variational DMRG calculation, of several benchmark problems: *ab initio* Hamiltonian of diamond, to Cr_2 dimer, two-dimensional 1-band and 3-band Hubbard models at half-filling in the strongly correlated regime of $U/t = 4-8$. More broadly, our work demonstrates new possibilities for efficiently accessing the ground state wavefunctions of highly correlated materials like transition metal oxides fully *ab initio* without recourse to approximate models.

ACKNOWLEDGMENTS

The calculations made use of the facilities of the Max Planck Society's Rechenzentrum Garching.

[1]P. Knowles and N. Handy, Chem. Phys. Lett. **111**, 315 (1984).
[2]S. R. White, Phys. Rev. Lett. **69**, 2863 (1992).
[3]S. R. White, Phys. Rev. B **48**, 10345 (1993).
[4]R. J. Bartlett and M. Musiał, Rev. Mod. Phys. **79**, 291 (2007).
[5]U. Schollwöck, Ann. Phys. **326**, 96 (2011).

[6]O. Legeza, R. M. Noack, J. Sólyom, and L. Tincani, in *Computational Many-particle Physics*, Lecture Notes in Physics Vol. 739, edited by H. Fehske, R. Schneider, and A. Weiße (Springer, Berlin Heidelberg, 2008), pp. 653–664.
[7]K. H. Marti and M. Reiher, Phys. Chem. Chem. Phys. **13**, 6750 (2011).
[8]Y. Kurashige and T. Yanai, J. Chem. Phys. **130**, 234114 (2009).
[9]S. R. White and R. L. Martin, J. Chem. Phys. **110**, 4127 (1999).
[10]S. Wouters and D. Van Neck, Eur. Phys. J. D **68**, 272 (2014).
[11]D. Zgid and M. Nooijen, J. Chem. Phys. **128**, 014107 (2008).
[12]G. H. Booth, A. Gruneis, G. Kresse, and A. Alavi, Nature **493**, 365 (2013).
[13]R. J. Bartlett, Ann. Rev. Phys. Chem. **32**, 32 (1981).
[14]W. D. Laidig and R. J. Bartlett, Chem. Phys. Lett. **104**, 424 (1984).
[15]W. D. Laidig, P. Saxe, and R. J. Bartlett, J. Chem. Phys. **86**, 887 (1987).
[16]R. F. Fink, Chem. Phys. Lett. **428**, 461 (2006).
[17]R. F. Fink, Chem. Phys. **356**, 39 (2009).
[18]T. Helgaker, P. Jorgensen, and J. Olsen, *Molecular Electronic-Structure Theory* (John Wiley & Sons, Inc., 2000).
[19]O. Sinanoğlu, J. Chem. Phys. **34**, 1237 (1961).
[20]E. Hylleraas, Z. Phys. **65**, 209 (1930).
[21]G. K. L. Chan and M. Head-Gordon, J. Chem. Phys. **116**, 4462 (2002).
[22]S. Sharma and G. K.-L. Chan, J. Chem. Phys. **136**, 124121 (2012).
[23]S. Sharma, J. Chem. Phys. **142**, 024107 (2015).
[24]S. Sharma and G. K.-L. Chan, J. Chem. Phys. **141**, 111101 (2014).
[25]F. A. Evangelista, M. Hanauer, A. Köhn, and J. Gauss, J. Chem. Phys. **136**, 204108 (2012).
[26]M. Hanauer and A. Köhn, J. Chem. Phys. **134**, 204111 (2011).
[27]K. R. Shamasundar, G. Knizia, and H.-J. Werner, J. Chem. Phys. **135**, 054101 (2011).
[28]J. Haegeman *et al.*, Phys. Rev. Lett. **107**, 070601 (2011).
[29]S. Wouters, N. Nakatani, D. Van Neck, and G. K.-L. Chan, Phys. Rev. B **88**, 075122 (2013).
[30]N. Nakatani, S. Wouters, D. Van Neck, and G. K.-L. Chan, J. Chem. Phys. **140**, 024108 (2014).
[31]T. Yanai, Y. Kurashige, E. Neuscamman, and G. K.-L. Chan, J. Chem. Phys. **132**, 24105 (2010).
[32]E. Neuscamman, T. Yanai, and G. K.-L. Chan, Int. Rev. Phys. Chem. **29**, 231 (2010).
[33]D. Ghosh, J. Hachmann, T. Yanai, and G. K. L. Chan, J. Chem. Phys. **128**, 144117 (2008).
[34]D. Zgid and M. Nooijen, J. Chem. Phys. **128**, 144115 (2008).
[35]D. J. Klein, J. Chem. Phys. **61**, 786 (1974).
[36]I. Shavitt and L. T. Redmon, J. Chem. Phys. **73**, 5711 (1980).
[37]B. H. Brandow, Rev. Mod. Phys. **39**, 771 (1967).
[38]M. Nooijen and J. G. Snijders, Int. J. Quantum Chem. **48**, 15 (1993).
[39]T. D. Kühner and S. R. White, Phys. Rev. B **60**, 335 (1999).
[40]E. Jeckelmann, Phys. Rev. B **66**, 045114 (2002).
[41]D. Cleland, G. H. Booth, C. Overy, and A. Alavi, J. Chem. Theory Comput. **8**, 4138 (2012).
[42]P. J. Knowles and H.-J. Werner, Chem. Phys. Lett. **145**, 514 (1988).
[43]H.-J. Werner and P. J. Knowles, J. Chem. Phys. **89**, 5803 (1988).
[44]H.-J. Werner, Mol. Phys. **89**, 645 (1996).
[45]C. Angeli, R. Cimiraglia, S. Evangelisti, T. Leininger, and J.-P. Malrieu, J. Chem. Phys. **114**, 10252 (2001).
[46]C. Angeli, R. Cimiraglia, and J.-P. Malrieu, Chem. Phys. Lett. **350**, 297 (2001).
[47]W. Purwanto, S. Zhang, and H. Krakauer, J. Chem. Phys. **142**, 064302 (2015).
[48]G. Li Manni, D. Ma, F. Aquilante, J. Olsen, and L. Gagliardi, J. Chem. Theory Comput. **9**, 3375 (2013).
[49]Y. Kurashige and T. Yanai, J. Chem. Phys. **135**, 094104 (2011).
[50]D. Zgid, D. Ghosh, E. Neuscamman, and G. K.-L. Chan, J. Chem. Phys. **130**, 194107 (2009).
[51]T. Müller, J. Phys. Chem. A **113**, 12729 (2009).
[52]C. Angeli, B. Bories, A. Cavallini, and R. Cimiraglia, J. Chem. Phys. **124**, 054108 (2006).
[53]P. Celani, H. Stoll, H.-J. Werner, and P. J. Knowles, Mol. Phys. **102**, 2369 (2004).
[54]H. Dachsel, R. J. Harrison, and D. A. Dixon, J. Phys. Chem. A **103**, 152 (1999).
[55]M. M. Goodgame and W. A. Goddard, Phys. Rev. Lett. **54**, 661 (1985).
[56]K. Andersson, B. Roos, P.-A. Malmqvist, and P.-O. Widmark, Chem. Phys. Lett. **230**, 391 (1994).
[57]C. W. Bauschlicher and H. Partridge, Chem. Phys. Lett. **231**, 277 (1994).
[58]H.-J. Werner, P. J. Knowles, G. Knizia, F. R. Manby, and M. Schütz, Wiley Interdiscip. Rev.: Comput. Mol. Sci. **2**, 242 (2012).
[59]R. Olivares-Amaya *et al.*, J. Chem. Phys. **142**, 034102 (2015).
[60]Z. Rolik, L. Szegedy, I. Ladjnszki, B. Ladczki, and M. Kllay, J. Chem. Phys. **139**, 094105 (2013).
[61]M. Kállay and P. R. Surján, J. Chem. Phys. **115**, 2945 (2001).
[62]G. Carleo, F. Becca, S. Moroni, and S. Baroni, Phys. Rev. E **82**, 046710 (2010).
[63]L. R. Schwarz, G. H. Booth, and A. Alavi, Phys. Rev. B **91**, 045139 (2015).
[64]G. H. Booth, A. J. W. Thom, and A. Alavi, J. Chem. Phys. **131**, 054106 (2009).
[65]D. Cleland, G. H. Booth, and A. Alavi, J. Chem. Phys. **132**, 041103 (2010).